Supramolecular Chemistry
Publication details, including instructions for authors and subscription information:
http://www.informaworld.com/smpp/title~content=t713649759

Determination of interaction strength between corrole and phenol derivatives in aqueous media using atomic force microscopy

Iwona Szymańska[a]; Eddy Dolusic[b]; Wim Dehaen[b]; Wouter Maes[b]; Takashi Ito[c]; Hanna Radecka[a]
[a] Institute of Animal Reproduction and Food Research of Polish Academy of Sciences, Tuwima, Olsztyn, Poland [b] Department of Chemistry, University of Leuven, Heverlee, Leuven, Belgium [c] Department of Chemistry, Kansas State University, Manhattan, KS, USA

To cite this Article Szymańska, Iwona , Dolusic, Eddy , Dehaen, Wim , Maes, Wouter , Ito, Takashi and Radecka, Hanna(2009) 'Determination of interaction strength between corrole and phenol derivatives in aqueous media using atomic force microscopy', Supramolecular Chemistry, 21: 7, 555 — 563
To link to this Article: DOI: 10.1080/10610270802406611
URL: http://dx.doi.org/10.1080/10610270802406611

Supramolecular Chemistry
Vol. 21, No. 7, October–November 2009, 555–563

Taylor & Francis
Taylor & Francis Group

Determination of interaction strength between corrole and phenol derivatives in aqueous media using atomic force microscopy

Iwona Szymańska[a], Eddy Dolusic[b], Wim Dehaen[b], Wouter Maes[b], Takashi Ito[c]* and Hanna Radecka[a]*

[a]*Institute of Animal Reproduction and Food Research of Polish Academy of Sciences, Tuwima, Olsztyn, Poland;* [b]*Department of Chemistry, University of Leuven, Leuven, Heverlee, Belgium;* [c]*Department of Chemistry, Kansas State University, Manhattan, KS, USA*

(*Received 20 June 2008; final version received 18 July 2008*)

Atomic force microscopy (AFM) was used to measure single interaction forces between corrole (host) and phenol derivatives (guests) in aqueous media. A gold tip was modified with thiol derivatives of corrole via the Au–S covalent bond. Such a tip was used to measure adhesion forces with a planar gold substrate modified with thiol derivatives of phenol and *ortho*-nitrophenol in aqueous solutions. The mean force between the corrole and *ortho*-nitrophenol was higher than that between corrole and phenol, probably reflecting stronger hydrogen bond interaction in the former complex. In the presence of a supporting electrolyte (0.1 M K_2SO_4), the mean force increased, suggesting that electrostatic and $\pi-\pi$ interactions play an essential role in the adhesion force. In addition, the adhesion force measured at pH 6.0 was larger than that at pH 10, reflecting the electrostatic repulsion at the higher pH. These behaviours are consistent with the potentiometric responses of a liquid membrane based on corrole to phenolic compounds. Also, the values of forces for the interaction between corrole and phenol derivatives showed the same tendency as energy calculated for these complexes. The Poisson method was used for the calculation of the single force of the chemical bond between the corrole host and the phenolic guests.

Keywords: atomic force microscopy; molecular recognition; corrole; phenol derivatives; aqueous media

Introduction

The exploring of the mechanism of the host–guest recognition at the molecular level is a valuable source of inspiration for researchers dealing with sensors that work by mimicking physiological processes occurring with outstanding sensitivity and selectivity. The source of the intensive development of the above study is a new research field, nanoscience, which deals with the objects as small as 1–100 nm (*1–2*). Images of surfaces at such an extremely small scale, down to resolving individual atoms or molecules, can be obtained by newly developed technologies, namely scanning tunnelling microscopy (STM) and atomic force microscopy (AFM) (*3–9*). The introduction of chemically tailored STM tips by Umezawa and co-workers dramatically improved the sensitivity of visualisation of molecular recognition processes at the membrane/solid interfaces (*10–18*). The chemical modification of STM tips (*10–18*) as well as AFM tips (*19*, *20*) increases the chemical affinity between the imaging tip and the substrates through the formation of hydrogen bonds, metal coordination bonds and charge transfer interactions. This remarkable cutting-edge technique has opened the possibility to explore the host–guest interactions at the molecular level between nucleobases (*18*), drug–enzyme (*21*), antigen–antibody (*22*, *23*) and other biomolecules (*24*, *25*), just to name a few.

The main objective of the research presented is showing the applicability of the AFM method together with chemically tailored tips for the exploring of the molecular recognition processes between corroles and phenol derivatives occurring at the solid/aqueous interface.

It has been already discovered by the potentiometric method that liquid membrane electrodes incorporating macrocyclic polyamines (*26–29*), calix[4]pyrroles (*30–33*) or corroles (*34–35*) upon stimulation with undissociated phenol derivatives generated potentiometric responses. The mechanism of this unusual phenomenon, generation of potentiometric signals by neutral molecules, relies on the transport of protons from the interface to the aqueous layer adjacent to the organic phase.

The host molecule being the subject of this study is corrole. This molecule belongs to the tetrapyrrolic macrocyclic compounds with 18π electrons. Corroles contain one direct linkage between two adjacent pyrrole rings. They display unusually high N–H acidity relative to other related macrocycles (*36*).

*Corresponding authors. Email: hanna.radecka@pan.olsztyn.pl; ito@ksu.edu

ISSN 1061-0278 print/ISSN 1029-0478 online

DOI: 10.1080/10610270802406611
http://www.informaworld.com

In this paper, we present a study on the interaction forces between corrole and phenol derivatives immobilised through Au–S bonds on a gold AFM tip and a gold substrate surface, respectively. The influence of the pH and the composition of aqueous solution on the strength of these interactions was also explored. These experiments have addressed the determination of type of forces between the corrole host and the phenolic guests, measured in aqueous media.

Experimental

Materials and reagents

The gold tip and substrate modification together with the chemical structures of the corrole and phenol derivatives used in the present study are illustrated in Scheme 1. Phenol and *ortho*-nitrophenol possessing the SH group were received from ProChimia Surfaces (Sopot, Poland). Planar gold substrates (Au.1000.ALSI) were purchased from Platypus Technologies (Madison, WI, USA). AFM cantilevers, commercially available (contact mode, resonant frequency 13 kHz, force constant 0.2 N/m), were obtained from Budgetsensors (Sofia Bulgaria). All aqueous solutions were prepared with deionised water purified with a Milli-Q water system. All the chemicals were of analytical grade, used as received.

Synthesis of corrole

Corrole was synthesised at the Department of Chemistry (University of Leuven) using method (*37–39*) as described below.

4-(10-Undecenoxy)benzaldehyde

A mixture of 7.030 g (28.64 mmol) of 11-bromo-1-undecene, 4.892 g (39.66 mmol) of *p*-hydroxybenzaldehyde and 8.328 g (60.26 mmol) of potassium carbonate was heated at reflux in 105 ml of acetone (p.a.) for 15 h. Upon cooling, the reaction mixture was filtered,

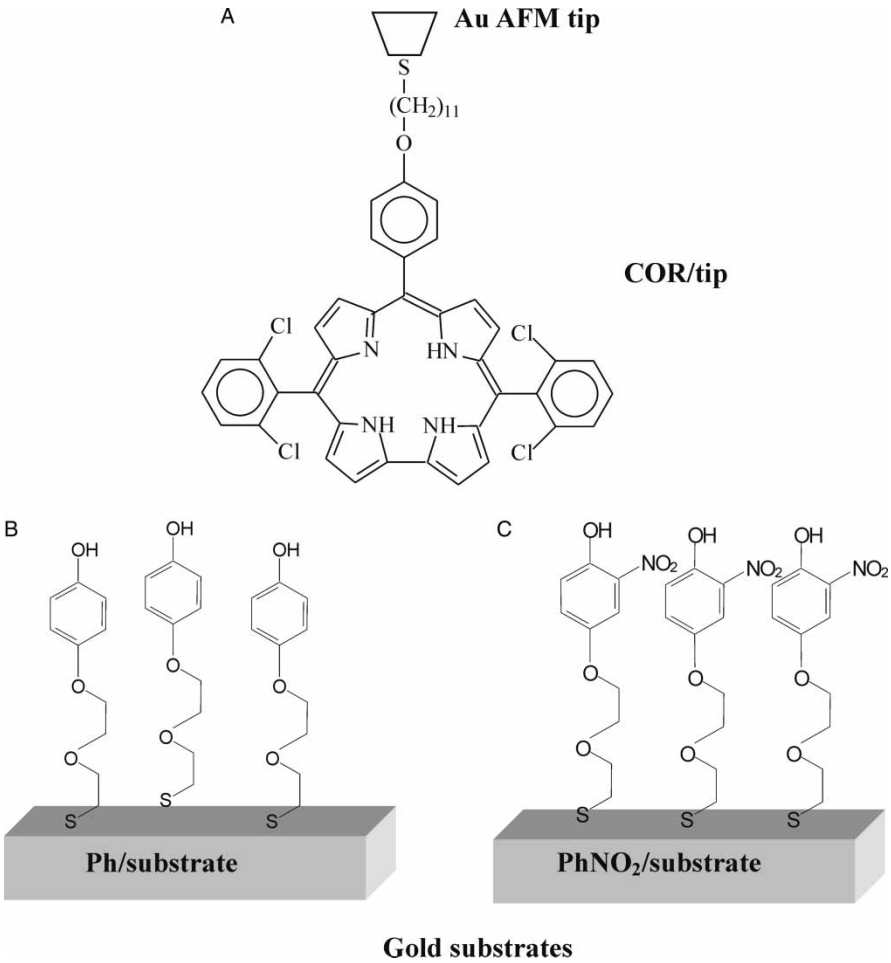

Scheme 1. Schematic of corrole–SH molecules (COR) immobilised on the surface of (A) a gold AFM tip, and (B) Ph and (C) $PhNO_2$ compounds immobilised on gold substrates.

evaporated to dryness and the residue was taken into dichloromethane. The solution was washed three times with aqueous NaOH, then three times with water and dried over $MgSO_4$. Upon filtration and removal of CH_2Cl_2 by distillation under reduced pressure, product **152** was purified by column chromatography on silica. Eluting with 1:1 dichloromethane/light petroleum ether afforded 7.450 g (95%) of the title product. δ_H (300 MHz) 9.88 (s, 1H, aldehyde H), 7.82 (d, *J* 8.1, 2H, aryl H), 6.99 (d, *J* 8.1, 2H, aryl H), 5.81 (m, 1H, undecenyl 10-H), 4.97 (m, 2H, undecenyl 11-H), 4.04 (t, *J* 6.6, 2H, undecenyl 1-H), 2.04 (q, *J* 7.0, 2H, undecenyl H), 1.81 (quintet, *J* 7.0, 2H, undecenyl 2-H), 1.46–1.31 (m, 12H, undecenyl H).

4-(11-Thioacetoxyundecyl)benzaldehyde

4-(10-Undecenoxy)benzaldehyde (7.450 g; 27.15 mmol), thioacetic acid (4 ml; 56.23 mmol) and azo-bis-isobutyronitrile (229 mg; 1.37 mmol) were dissolved in 90 ml of toluene (p.a.). The mixture was degassed with a stream of argon and then refluxed for 6.5 h. The reaction was quenched with 5% aqueous $NaHCO_3$ (400 ml) and extracted three times with ethyl acetate. The combined organic layers were washed with 5% aqueous $NaHCO_3$, then brine and dried over $MgSO_4$. Upon filtration and removal of the solvent under reduced pressure, the yellow solid residue was chromatographed on silica eluting with a gradient of 5:1–1:1 light petroleum ether/ethyl acetate. The crude product obtained was recrystallised from methanol to afford 4.086 g (43%) of a white powder. δ_H (300 MHz) 9.88 (s, 1H, aldehyde H), 7.83 (d, *J* 8.6, 2H, aryl H), 6.99 (d, *J* 8.6, 2H, aryl H), 4.04 (t, *J* 6.6, 2H, undecenyl 1-H), 2.86 (t, *J* 7.3, 2H, undecenyl 11-H), 2.32 (s, 3H, CH_3), 1.81 (quintet, *J* 7.3, 2H, undecenyl 2-H), 1.46–1.28 (m, 16H, $8CH_2$).

Meso-5,15-bis(2,6-dichlorophenyl)-10-(4-(11-thioacetoxy-1-dodecyloxy)phenyl)corrole

2,6-Dichlorophenyldipyrromethane (1.522 g; 5.23 mmol) and 4-(11-thioacetoxyundecyl)benzaldehyde (606 mg; 1.73 mmol) were dissolved in 146 ml of dichloromethane. The reaction flask was wrapped in aluminium foil and placed in an ice bath. The solution was bubbled with Ar for 15 min. Ten microlitres of TFA (0.13 mmol) was added and the mixture was stirred under an argon atmosphere for ~48 h. The ice bath was removed and 935 mg (3.77 mmol) of *p*-chloranil was added. After additional 1 h at room temperature, the mixture was evaporated with silica and chromatographed twice in a 1.5:1 mixture of dichloromethane and *n*-heptane to afford 452 mg (29%) of corrole. δ_H 9.00 (d, *J* 4.1, 2H, 2-H and 18-H of corrole), 8.62 (d, *J* 4.7, 2H, 8-H and 12-H of corrole), 8.53 (d, *J* 4.7, 2H, 7-H and 13-H of corrole), 8.42 (d, *J* 4.1, 2H, 3-H and 17-H of corrole), 8.08 (d, *J* 8.5, 2H, aryl *o*-H), 7.78 (d, *J* 7.7, 4H, dichlorophenyl *m*-H), 7.66 (dd, J_1 7.7, J_2 8.7, 2H, dichlorophenyl *p*-H), 7.27 (d partially overlapped with $CHCl_3$, *J* 8.5, 2H, aryl *m*-H), 4.24 (t, *J* 6.5, 2H, OCH_2), 2.89 (t, *J* 7.3, 2H, SCH_2), 2.32 (s, 3H, CH_3), 1.98 (quintet, *J* 7.4, 2H, β-CH_2), 1.62–1.36 (m, 16H, $8CH_2$), −2.30 (br. s, 3H, NH); δ_C 196.0, 158.9, 138.6 (quaternary C), 137.4 (quaternary C), 135.5 (CH), 134.0 (quaternary C), 130.3 (dichlorophenyl *p*-C), 128.0 (dichlorophenyl *m*-C), 127.2 (pyrrole CH), 125.7 (pyrrole CH), 120.8 (C-3 and C-17 of corrole), 116.2 (C-2 and C-18 of corrole), 113.2 (CH), 111.7 (quaternary C), 108.8 (quaternary C), 68.3, 30.6, 29.6, 29.5, 29.1, 28.8, 26.2; UV–Vis 410.1 (1.35×10^5), 566.1 (0.22×10^5); ESI-MS 907 (MH^+).

Meso-5,15-bis(2,6-dichlorophenyl)-10-(4-(11-mercapto-1-dodecyloxy)phenyl)corrole

Acetyl-protected corrole (130 mg; 0.14 mmol) was dissolved in 7.5 ml of THF and 3 ml of methanol. The flask was placed in an ice bath and 1 ml of a 1.65 M solution of CH_3ONa in methanol (1.65 mmol of CH_3ONa) was added. The reaction mixture was stirred at 0°C for 30 min and then poured into diluted aqueous HCl (~0.02 M). This solution was extracted with ethyl acetate (some brine had to be added for a better separation), and then washed with brine, distilled water and dried over $MgSO_4$. Upon filtration and removal of the solvent under reduced pressure, 26 mg (21%) of corrole thiol was isolated by chromatography in mixtures of CH_2Cl_2 and hexane (1.5:1, column and 1:1, preparative plate). δ_H 8.97 (d, *J* 3.9, 2H, 2-H and 18-H of corrole), 8.61 (d, *J* 4.5, 2H, 8-H and 12-H of corrole), 8.51 (d, *J* 4.5, 2H, 7-H and 13-H of corrole), 8.39 (d, *J* 3.9, 2H, 3-H and 17-H of corrole), 8.07 (d, *J* 8.2, 2H, aryl *o*-H), 7.72 (m, 4H, dichlorophenyl *m*-H), 7.59 (dd, J_1 8.3, J_2 8.3, 2H, dichlorophenyl *p*-H), 7.24 (d partially overlapped with $CHCl_3$, *J* 8.2, 2H, aryl *m*-H), 4.20 (t, *J* 6.4, 2H, OCH_2), 2.50 (t, *J* 6.8, 2H, SCH_2), 1.93 (quintet, 2H, β-CH_2), 1.60 (m, 4H, $2CH_2$), 1.39–1.26 (m, 13H, $6CH_2$ and SH), ~ −1.9 (br. s, 3H, NH); δ_C 158.8 (CO), 142.1 (9-C and 11-C of corrole), 139.8 (6-C and 14-C of corrole), 138.5, 137.4, 135.5, 134.6, 134.0, 130.7, 130.3, 128.0 (3-C and 5-C of 5,15-dichlorophenyl), 127.1, 125.7 (8-C and 12-C of corrole), 120.8 (A and D ring β-pyrrole C), 116.2 (A and D ring β-pyrrole C), 113.2 (A and D ring β-pyrrole C), 111.7 (5-C and 15-C of corrole), 108.9 (10-C of corrole); ESI-MS 865 (MH^+).

Formation of SAMs on gold substrates and gold tips

Before the modification, the substrates were sonicated for 10 min in ethanol, dried with argon and annealed in a hydrogen flame. Next, the gold substrates were immersed in 10 mM ethanolic solutions of derivatives of phenol (Ph)

and nitrophenol ($PhNO_2$), for 20 h. Next, the substrates were rinsed with ethanol and water and dried in air. At least, three repetitions of the substrate modification samples were done.

The gold tips were washed with ethanol, pretreated in an UV/ozone chamber (Novascan Technologies, Ames, USA) for 30 min and then immersed in 0.5 mM corrole (COR) chloroform solution for 24 h. Thus, five tips were modified and used for the experiments.

AFM measurements

AFM measurements were carried out with a Molecular Imaging PicoSPM (Agilent Technologies, Tempe, USA). Substrates Ph or $PhNO_2$ and cantilever COR/tip were loaded in a liquid cell, which was allowed to reach thermal equilibrium before starting the AFM operation. Adhesion forces were determined from force–displacement curves at room temperature (*ca* 20°C) with the substrate and tip immersed in, Milli-Q water, an aqueous solution containing 0.1 M K_2SO_4 at pH 6.0 or 10.0, using the scanning rate of 1.17 lines/s. For each combination of tip and substrates, and appropriate pH of solution, at least 300 force–displacement curves were measured at different positions of each substrate–tip combination.

Results and discussion

Strength of the adhesion forces between the corrole host and the phenolic guests measured in water by AFM

The experiments to study the interactions between the corrole host and the phenolic guests were carried out by using modified gold substrates and tips. The modification procedures are illustrated in Scheme 1.

First, interactions between a COR/tip and Ph- or $PhNO_2$/substrates were assessed in water at room temperature. The tip and substrate were mounted in liquid cell and the force–displacement curves were monitored. Figure 1 shows a typical force–displacement curve observed between a $PhNO_2$/substrate and a COR/tip. In many measurements, an adhesion force as shown in Figure 1 was observed in the retracting part of the curve. In this paper, the host–guest interactions in water will be verified based on adhesion force, since it has often been used to discuss various intermolecular interactions (*40*). Adhesion forces obtained from multiple measurements using a single tip on different locations of a sample were summarised in a histogram, which show the probability of a given value of adhesion forces. Figures 2(A) and 3(A) show histograms observed with a COR/tip on a Ph/substrate and a $PhNO_2$/substrate, respectively. The average of the adhesion force, measured using multiple COR/tips, was slightly larger for the $PhNO_2$/substrates (2.1 ± 0.5 nN) in comparison with the Ph/substrate (1.7 ± 0.3 nN) (Table 1).

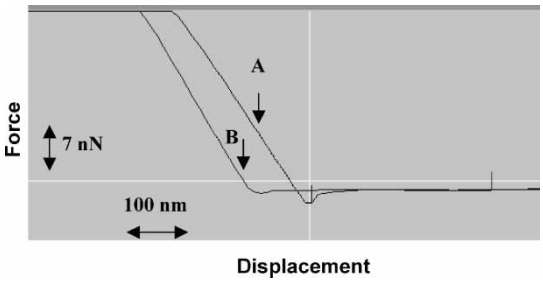

Figure 1. Typical force curves (line 'B', approaching; line 'A', retracting) observed for $PhNO_2$/substrates using COR/tip made in water.

In order to assess the contribution of non-specific interactions to the aforementioned adhesion force data, force–distance curves on Ph- or $PhNO_2$/substrates were measured using unmodified gold tip. Figure 4(A) and 4(B) shows histograms obtained from the adhesion force data for a single tip. The adhesion forces were 1.0 ± 0.2 nN and 0.7 ± 0.2 nN, for Ph- and $PhNO_2$/substrates, respectively. These values were smaller than those obtained with COR/tip. In addition, bare gold tips gave slightly larger adhesion force on Ph/substrates, whereas COR/tips gave

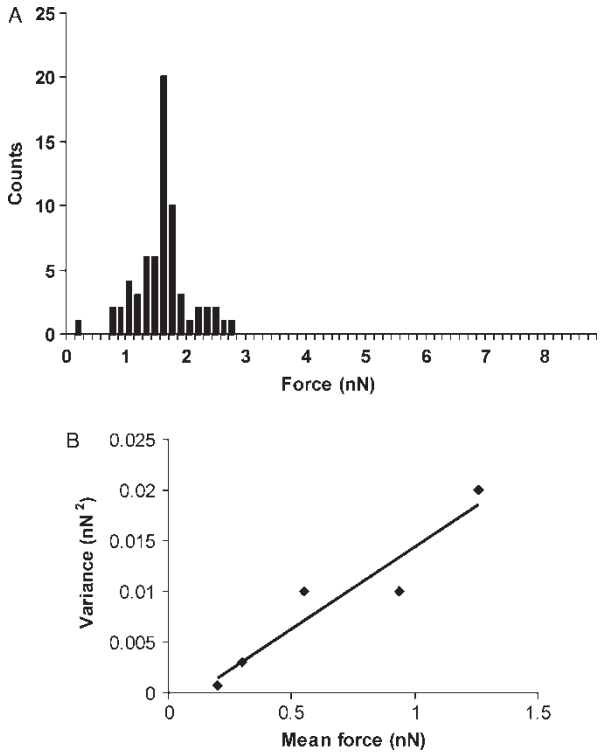

Figure 2. (A) A histogram of adhesion forces obtained from the repetitive force measurements between a single COR/tip and a Ph/substrate in water. (B) A plot of mean vs. variance of the adhesion force measured for Ph/substrates using five separate COR/tips in water.

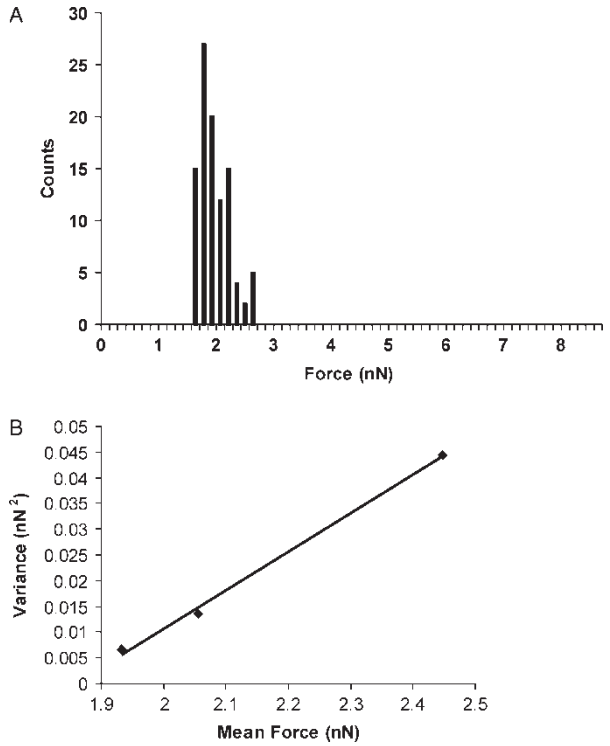

Figure 3. (A) A histogram of adhesion forces obtained from the repetitive force measurements between a single COR/tip and a $PhNO_2$/substrate in water. (B) A plot of mean vs. variance of the adhesion force measured for $PhNO_2$/substrates using three separate COR/tips in water.

larger force on $PhNO_2$/substrate. These results suggest that the difference in the adhesion force measured using COR/tips reflects from the host–guest interactions.

The adhesion force reported above reflects not only the host–guest interactions but also the contact area originating from the variation in tip size (*41*). The pull-off features in the retracting part of the force–distance curve can also be used to calculate the strength of a single chemical bond (*42–46*), which is not affected by the variation of the contact area. It has already been reported that AFM contact forces obeyed a Poisson distribution. Thus, the ratio of their variance to the mean gives the force of a single chemical bond between the tip

Table 1. Adhesion forces measured with unmodified and corrole-modified tips and gold substrates modified with Ph or $PhNO_2$ in different aqueous solutions.

	Ph/substrate (nN)	$PhNO_2$/substrate (nN)
Unmodified tip, water	1.0 ± 0.2	0.7 ± 0.2
COR/tip, water	1.7 ± 0.3	2.1 ± 0.5
COR/tip, 0.1 M K_2SO_4, pH 6.0	2.2 ± 0.6	5.0 ± 0.8
COR/tip, 0.1 M K_2SO_4, pH 10.0	0	0

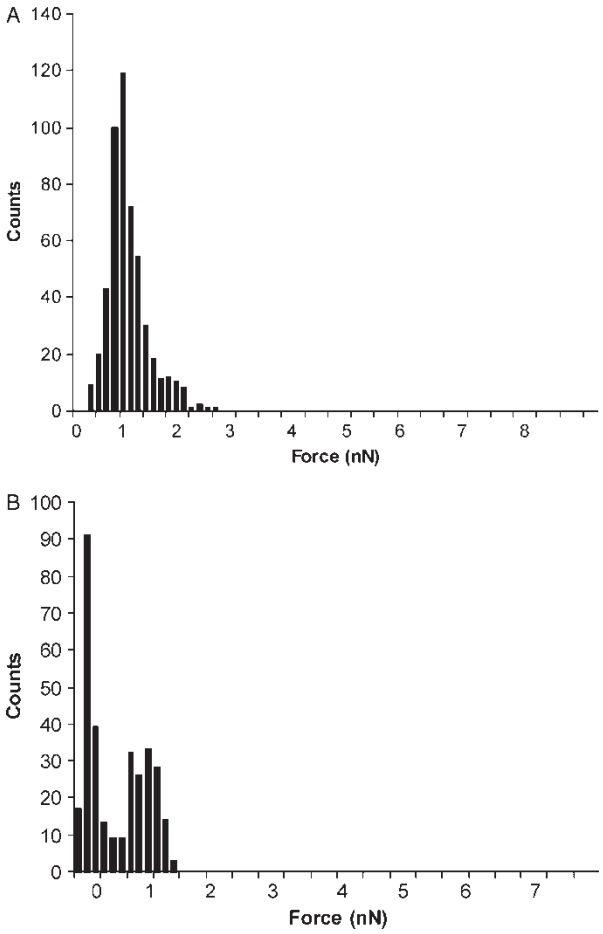

Figure 4. Histograms of adhesion forces ($n = 300$) obtained from the repetitive force measurements between a bare gold AFM tip and (A) a Ph/substrate and (B) a $PhNO_2$/substrate in water.

and the substrate. The Poisson method requires relatively few measurements. By plotting a linear regression curve of the variance vs. the mean force taken from several sets of AFM measurements performed at different locations on the surface and different tips, the magnitude of the individual bond force can be estimated. The lack of assumptions about the tip radius is another important advantage of this method. Indeed, the Poisson statistical analysis method has been widely used for the calculation of individual bond forces between the AFM tip and the substrate, both functionalised (*42–46*). Thus, the Poisson method was used in the present study for the evaluation of the strength of single molecule bond forces between corrole and phenol or *ortho*-phenol derivatives. Corroles due to the steric hindrance create less packed monolayers on the surface. Moreover, because of the presence of short ethylene chains, the phenol derivatives SAMs are less ordered. These factors cause that the density of the host and guest on the surface is rather low. Thus, the Poisson method is suitable for the systems studied.

From the slope of the linear relationship between the mean force and its variance, the single molecule bond force can be calculated (Figures 2(B) and 3(B)). The calculated single molecule bond forces were 16 ± 3 pN for the Ph- and 75 ± 11 pN for the $PhNO_2$/substrate, respectively (Table 2). Thus, the strength of the individual bond force between corrole and *ortho*-nitrophenol was almost five times higher in comparison with the force between corrole and phenol. These values are in a similar range as reported by Beebe et al. (*42*) and van der Vegte and Hadziioannou (*47*). Their reports deal with a study of the hydrogen bonding, van der Waals and Coulombic interactions between *ω*-functional *n*-alkanethiol compounds with a variety of functional groups (CH_3, OH, NH_2, COOH and $CONH_2$), which were used for the modification of scanning force microscopy probes and substrates.

pH dependence on the strength of the adhesion forces between the corrole host and the phenolic guests measured in 0.1 M K_2SO_4 by the AFM method

In order to explore the influence of the pH and the electrolyte on the strength of interactions between the host and the guests studied, subsequent experiments were performed in the presence of 0.1 M K_2SO_4 at two pH values 6.0 and 10.0.

At pH 6.0, the shape of the force–distance curves was similar to that observed in water (Figure 1). At that pH, corrole exists as a mixture of electrically neutral and deprotonated molecules on the surface of the gold tip (*34*). On the other hand, the phenol and *ortho*-nitrophenol derivatives exist as the undissociated compound (*31*, *32*).

The histograms for the adhesion forces obtained for COR/tip and Ph- or $PhNO_2$/substrate measured at pH 6.0 and their corresponding plots of mean force vs. variance are given in Figures 5 and 6, respectively. The average of the adhesion force of COR/tips with $PhNO_2$/substrates (5.0 ± 0.8 nN; Figure 6(A) and Table 1) is twice larger than that with Ph/substrates (2.2 ± 0.6 nN; Figure 5(A) and Table 1). The single bond force between corrole and $PhNO_2$ was also larger (140.5 ± 33.0 pN; Figure 6(B) and Table 2) than that between corrole and Ph (59.3 ± 10 pN; Figure 5(B) and Table 2). This result is again consistent with the stronger interactions between the corrole molecules and *ortho*-nitrophenol in comparison with phenol.

Table 2. Single bond forces measured with corrole-modified tips and Ph and $PhNO_2$ compounds immobilised on gold substrates in different aqueous solutions.

	Ph/substrate (pN)	$PhNO_2$/substrate (pN)
COR/tip, water	16.1 ± 3.0	75.1 ± 11
COR/tip, 0.1 M K_2SO_4, pH 6.0	59.3 ± 10.0	140.5 ± 33.0
COR/tip, 0.1 M K_2SO_4, pH 10.0	0	0

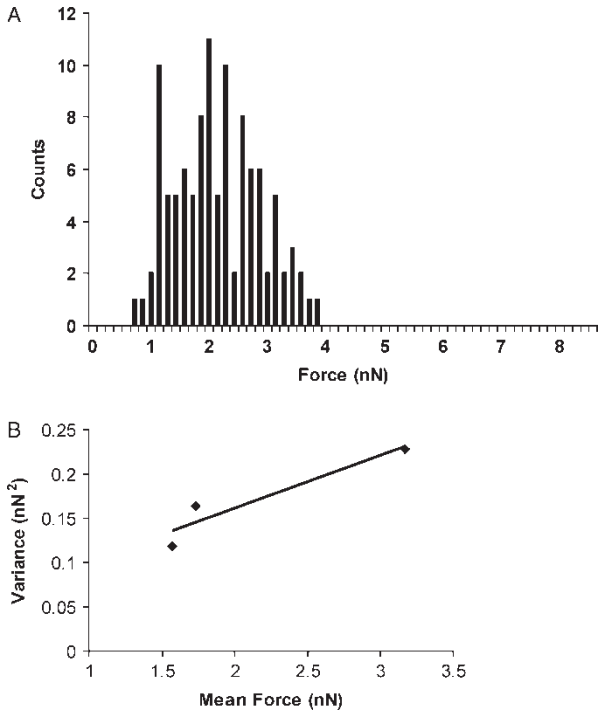

Figure 5. (A) A histogram of adhesion forces obtained from the repetitive force measurements between a single COR/tip and a Ph/substrate in 0.1 M K_2SO_4 (pH 6.0). (B) A plot of mean vs. variance of the adhesion force measured for Ph/substrates using three separate COR/tips in 0.1 M K_2SO_4 (pH 6.0).

The adhesion force between the tip modified with corrole and substrates was not observed at pH 10 (Figure 7). The recorded force–distance curves displayed the typical shape for the repulsive forces between the functionalised tip and the surface (*40*). This lack of adhesion force is mainly caused by the electrostatic repulsion between the tip and the substrate. At pH 10.0, both corrole molecules and phenol and *ortho*-nitrophenol derivatives exist in the negatively charged forms. The pK_as of *ortho*-nitrophenol and phenol are 7.21 and 10.0, respectively. Thus, at pH 10.0, both the host and guests molecules obtain a negative charge.

Similar phenomena, namely the switching in binding forces in relation to a change in the pH, were observed in several studies. The deprotonation effect of the ammonium group on the surface of the substrate under basic condition caused a decrease in the interaction between ammonium ion complexes with crown ethers moiety, as presented by Kimura et al. (*48*). A decrease in the adhesion force with increased H^+ concentration for amino- or 2-imidazolin-1-yl-terminated SAMs is a result of the repulsion between the positively charged tip and the substrate surfaces, as reported by Umezawa and co-workers (*49*). In the present study, we have demonstrated that the individual interaction forces between corrole and phenol as well as *ortho*-nitrophenol derivatives attached to the surface of a gold tip

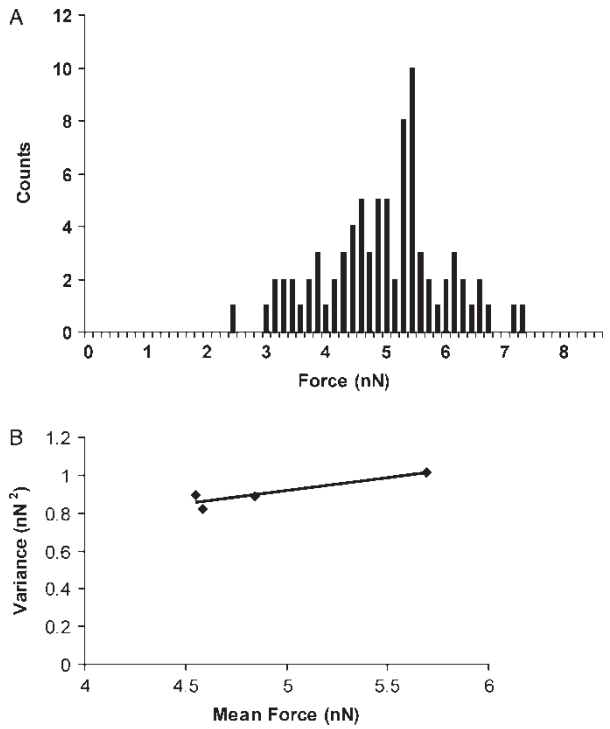

Figure 6. (A) A histogram of adhesion forces obtained from the repetitive force measurements between a single COR/tip and a $PhNO_2$/substrate in 0.1 M K_2SO_4 (pH 6.0). (B) A plot of mean vs. variance of the adhesion force measured for $PhNO_2$/substrates using four separate COR/tips in 0.1 M K_2SO_4 (pH 6.0).

and gold substrates depend on the protonation/deprotonation conditions of both the host and the guests. By changing the pH of the electrolyte solutions, switching in the binding force is possible. As summarised in Table 2, the strongest single bond force was observed between the corrole and the *ortho*-nitrophenol derivatives measured at pH 6.0. The presence of the electrolyte, 0.1 M K_2SO_4, increased the strength of the interactions, approximately four times for corrole–phenol, and two times for corrole–*ortho*-nitrophenol, in comparison with the values obtained in pure water. The larger adhesion force in the presence of 0.1 M K_2SO_4 suggests the involvement of hydrophobic interactions (e.g. $\pi-\pi$ interactions) in the supramolecular complex formed between corrole and phenols.

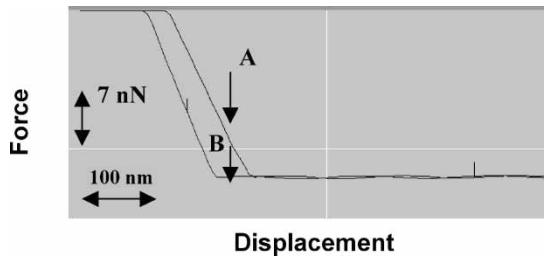

Figure 7. Typical force curves (line 'B', approaching; line 'A', retracting) observed for $PhNO_2$/substrates using COR/tip made in 0.1 M K_2SO_4 at pH 10.0.

Computer simulation on the complexation between corrole and phenols

In addition, the difference in the adhesion force observed for $PhNO_2$- and Ph/substrate would originate from hydrogen bond interactions with corrole. The creation of supramolecular assemblies is controlled by N–H···X and O–H···X (X = O, N) hydrogen bonds. The majority of recent publications are connected with molecular complexes of phenolic substrates with a variety of receptors (*50*, *51*). These reports show that the supramolecular assembly is controlled by strong and directional O–H···N hydrogen bonds. The phenolic compounds can create a supramolecular complex with corrole (*33*, *34*). The interaction involves the creation of a hydrogen bond between the NH group of the macrocyclic cavity of the corrole and the OH group of the phenol derivative. The oxygen from the phenolic host is an acceptor of hydrogen, while the NH group is a donor of hydrogen.

The significance of the hydrogen bond interactions in the host–guest supramolecular complex was verified using the AM1 geometry procedure (MOPAC 2002 Version 2.5.3, J.J.P. Stewart, Fujitsu Limited, Tokyo, Japan). The calculation of a number of different conformations of the corrole and guest compounds was performed using the CaChe Workspace programme in vacuum (CaChe Worksystem Pro Version 7.5.0.85). In Scheme 2, a model of the complex formation between the corrole and the *ortho*-nitrophenol derivatives is presented, as optimised by the AM1 geometry procedure. However, the calculation showed that the binding energy of *ortho*-nitrophenol is in a range of -5.8 kcal/mol. On the other hand, the phenol binding strength is a little less energetically favourable (-3.5 kcal/mol). In order to correlate the energy binding and force of the complex formation of corrole with phenol and *ortho*-nitrophenol, the procedure described by Reinhoudt was applied (*52*). In this procedure, the dependence of pull-off forces vs. energy was achieved for the spherical and cylindrical integration approaches, according to the following equations: $F = 32.60 \times \sqrt{-\Delta G + 2.39}$ or $F = 31.76 \times \sqrt{-\Delta G + 1.03}$, respectively (with $-\Delta G$ in kcal/mol and F in pN). Taking into account cylindrical integration approaches, the calculated values of forces were 83.0 pN and 67.6 pN, for $PhNO_2$ and Ph, respectively. The difference between predicted and experimental values is therefore as follows: 83.0/140.5 and 67.6/59.3 pN, respectively, when compared with the values obtained in 0.1 K_2SO_4, pH 6.0. The differences between calculated and experimental data could be caused by possible contribution of other kind of forces (e.g. $\pi-\pi$ interactions or hydration of water molecules to the complex). However, the results of calculation show the similar tendency as experimental data described in this paper.

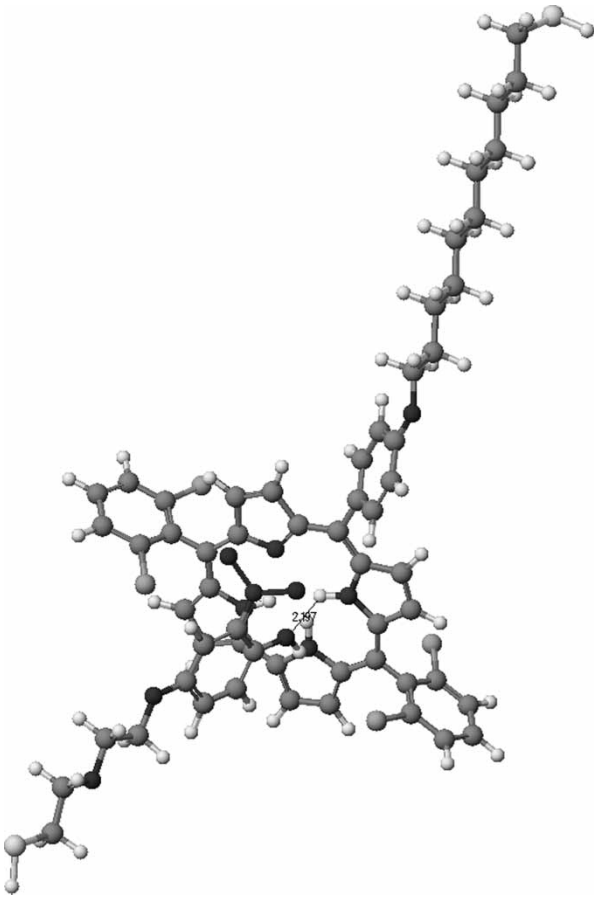

Scheme 2. Structure of the complex between corrole and an *ortho*-nitrophenol derivative optimised by the AM1 geometry procedure (CaChe Worksystem Pro Version 7.5.0.85).

The results obtained using AFM together with a chemically modified tip also correlate well with those obtained potentiometrically, which concern the studies of corroles as the selective receptors for phenol derivatives existing as the electrically neutral analytes (*33–35*). The presence of a nitro group on the benzene ring increases the acidity of the phenolic OH group, and, as a consequence, a stronger potentiometric signal was observed. The significant part of the recognition process is the formation of weak hydrogen bonds between the electron pairs of the phenolic OH group and the NH units belonging to the corrole. This phenomenon was proved here, at the molecular level, by the AFM method together with a chemically modified tip and substrates.

Conclusions

We presented a study on the strength of the interactions between a corrole host and phenolic guests using the AFM method together with gold substrates and tips modified with SAMs thorough Au–S covalent bonds. The specific intermolecular forces between corrole covalently immobilised on the gold AFM tip and derivatives of phenol, also attached via a sulphur–gold bond to the surface of substrates, were observed by means of AFM. The dominant nature in the selectivity of interactions between the corrole host and the phenolic guests are hydrogen bonds. Also, hydrophobic and $\pi-\pi$ interactions between phenol and pyrrole rings are involved. The strength of the single adhesion forces between the corrole host and the phenolic guests was determined by the Poisson method analysis. The sequence of the strength of the single bond force obtained with the AFM method correlates well with the calculated values of energy and the selectivity of potentiometric signals obtained by liquid membrane electrodes incorporating corrole after stimulation with neutral phenolic guests (*33–35*). The results obtained confirm the possibility of applying the AFM for the observation at the molecular level of the creation of supramolecular complexes between nitrogen-containing macrocycles and uncharged phenol derivatives. Notably, the nitrophenol isomers were recently identified as vasodilators which can mimic hormones, and can be considered as endocrine disrupting chemicals possessing estrogenic activity (*53*). Thus, looking for the compounds that could specifically bind these molecules is very important from the theoretical and practical point of view. On the other hand, taking into account the interesting features of corrole, which might be protonated and associate with a low pH cancer cell, these molecules can be used as sensors in biological systems and therefore there is still need for basic research connected with analogous systems.

Acknowledgements

We gratefully acknowledge financial support from the Kościuszko Foundation (to I. Szymańska), EU grant COST D31/0021/05 (to I. Szymańska, H. Radecka, E. Dolusic, W. Dehaen and W. Maes), Polish Ministry of Science and Higher Education 19/COS/2006/3 (to I. Szymańska and H. Radecka), the F.W.O., the University of Leuven and the Ministerie voor Wetenschapsbeleid (to E. Dolusic, W. Dehaen and W. Maes) and Kansas State University (to T. Ito).

References

(1) Joachim, C. *Nat. Mater.* **2005**, *4*, 107–109.
(2) Love, J.Ch.; Estroff, L.A.; Kriebel, J.K.; Nuzzo, R.G.; Whitesides, G.M. *Chem. Rev.* **2005**, *105*, 1103–1169.
(3) Skoog, D.A.; Holler, F.J.; Nieman, T.A. Thomson Learning, 5th ed.; 1998.
(4) Sugimoto, Y.; Abe, M.; Hirayama, S.; Oyabu, N.; Custance, O.; Morita, S. *Nat. Mater.* **2005**, *4*, 156–159.
(5) Kuffer, O.R.; Maggio-Aprile, I.; Fisher, O. *Nat. Mater.* **2005**, *4*, 378–382.
(6) Mikkelsen, A.; Skold, N.; Ouattara, L.; Borgstrom, M.; Andersen, J.N.; Samuelson, L.; Seifert, W.; Lundgren, E. *Nat. Mater.* **2004**, *3*, 519–523.

(7) Tromas, Ch.; Eaton, P.; Mimault, J.; Rojo, J.; Penadés, S. *Langmuir* **2005**, *21*, 6142–6144.
(8) Podoprygorina, G.; Janke, M.; Janshoff, A.; Bohmer, V. *Supramol. Chem.* **2008**, *20*, 59–69.
(9) Sansone, F.; Baldini, L.; Casnati, A.; Ungaro, R. *Supramol. Chem.* **2008**, *20*, 161–168.
(10) Ito, T.; Bühlmann, P.; Umezawa, Y. *Anal. Chem.* **1998**, *70*, 255–259.
(11) Ito, T.; Bühlmann, P.; Umezawa, Y. *Anal. Chem.* **1999**, *71*, 1699–1705.
(12) Nishino, T.; Bühlmann, P.; Ito, T.; Umezawa, Y. *Phys. Chem. Chem. Phys.* **2001**, *3*, 1867–1869.
(13) Nishino, T.; Bühlmann, P.; Ito, T.; Umezawa, Y. *Surf. Sci.* **2001**, *490*, L579–L584.
(14) Odashiro, T.; Ito, T.; Bühlmann, P.; Umezawa, Y. *Anal. Chem.* **2001**, *73*, 878–883.
(15) Nishino, T.; Ito, T.; Umezawa, Y. *Anal. Chem.* **2002**, *74*, 4275–4278.
(16) Nishino, T.; Ito, T.; Umezawa, Y. *J. Electroanal. Chem.* **2003**, *550*, 125–129.
(17) Nishino, T.; Ito, T.; Umezawa, Y. *Proc. Natl. Acad. Sci. USA* **2005**, *102*, 5659–5662.
(18) Ohshiro, T.; Umezawa, Y. *Proc. Natl. Acad. Sci. USA* **2006**, *103*, 10–14.
(19) Han, T.; Williams, J.M.; Beebe, T.P., Jr. *Anal. Chim. Acta* **1995**, *307*, 365–376.
(20) Ito, T.; Namba, M.; Buhlmann, P.; Umezawa, Y. *Langmuir* **1997**, *13*, 4323–4332.
(21) Rigby-Singleton, S.M.; Allen, S.; Davies, M.C.; Roberts, C.J.; Tendler, S.J.B.; Williams, P.M.J. *Chem. Soc. Perkin Sens.* **2002**, *2*, 1722–1727.
(22) Browning-Kelley, M.E.; Wadu-Mesthrige, K.; Hari, V.; Liu, G.Y. *Langmuir* **1997**, *13*, 343–350.
(23) Avci, R.; Schweitzer, M.; Boyd, R.D.; Wittmeyer, J.; Steele, A.; Toporski, J.; Beech, I.; Teran Arce, F.; Spangler, B.; Cole, K.M.; McKay, D.S. *Langmuir* **2004**, *20*, 11053–11063.
(24) Basnar, B.; Elnathan, R.; Willner, I. *Anal. Chem.* **2006**, *78*, 3638–3642.
(25) Janshoff, A.; Neitzert, M.; Oberdorfer, Y.; Fuchs, H. *Angew. Chem., Int. Ed.* **2000**, *39*, 3212–3237.
(26) Piotrowski, T.; Szymańska, I.; Radecka, H.; Radecki, J.; Pietraszkiewicz, M.; Pietraszkiewicz, O.; Wojciechowski, K. *Electroanalysis* **2000**, *12*, 1397–1402.
(27) Ito, T.; Radecka, H.; Tohda, K.; Odashima, K.; Umezawa, Y. *J. Am. Chem. Soc.* **1998**, *120*, 3049–3059.
(28) Ito, T.; Radecka, H.; Umezawa, K.; Kimura, T.; Yashiro, A.; Lin, X.M.; Kataoka, M.; Kimura, E.; Sessler, J.L.; Odashima, K.; Umezawa, Y.A. *Anal. Sci.* **1998**, *14*, 89–98.
(29) Odashima, K.; Naganawa, R.; Radecka, H.; Kataoka, M.; Kimura, E.; Koike, T.; Tohda, K.; Tange, M.; Furuta, H.; Sessler, J.L.; Yagi, K.; Umezawa, Y. *Supramol. Chem.* **1994**, *4*, 101–113.
(30) Piotrowski, T.; Radecka, H.; Radecki, J.; Depraetere, S.; Dehaen, W. *Mater. Sci. Eng., C* **2001**, *18*, 223–228.
(31) Piotrowski, T.; Radecka, H.; Radecki, J.; Depraetere, S.; Dehaen, W. *Electroanalysis* **2001**, *13*, 342–346.
(32) Radecki, J.; Radecka, H.; Piotrowski, T.; Depraetere, S.; Dehaen, W.; Plavec, J. *Electroanalysis* **2004**, *16*, 2073–2081.
(33) Radecki, J.; Dehaen, W. *Comb. Chem. High Throughput Screening* **2006**, *9*, 399–406.
(34) Radecki, J.; Stenka, I.; Dolusic, E.; Dehaen, W.; Plavec, J. *Comb. Chem. High Throughput Screening* **2004**, *7*, 375–381.
(35) Radecki, J.; Stenka, I.; Dolusic, E.; Dehaen, W. *Electrochim. Acta* **2006**, *51*, 2282–2288.
(36) Mahammed, A.; Gray, H.B.; Weaver, J.; Gross, Z. *Tetrahedron Lett.* **2003**, *44*, 2077–2079.
(37) Asokan, C.V.; Smeets, S.; Dehaen, W. *Tetrahedron Lett.* **2001**, *42*, 4483–4485.
(38) Maes, W.; Ngo, T.N.; Vanderhaeghen, J.; Dehaen, W. *Org. Lett.* **2007**, *9*, 3165–3168.
(39) Rohand, T.; Dolusic, E.; Ngo, T.H.; Maes, W.; Dehaen, W. *Arkivoc* **2007**, 307–324.
(40) Janshoff, A.; Neitzert, M.; Oberdorfer, Y.; Fuchs, H. *Angew. Chem., Int. Ed.* **2000**, *39*, 3212–3237.
(41) Israelachvili, J.N. *Intermolecular and Surface Forces*; Academic: London, 1985.
(42) Han, T.; Williams, J.M.; Beebe, T.P., Jr. *Anal. Chim. Acta* **1995**, *307*, 365–376.
(43) Stevens, F.; Lo, Y.-S.; Harris, J.M.; Beebe, T.P.,Jr. *Langmuir* **1999**, *15*, 207–213.
(44) Lo, Y.-S.; Zhu, Y.-J.; Beebe, T.P., Jr. *Langmuir* **2001**, *17*, 3741–3748.
(45) Lo, Y.- S.; Huefner, N.D.; Chan, W.S.; Stevens, F.; Harris, J.M.; Beebe, T.P., Jr. *Langmuir* **1999**, *15*, 1373–1382.
(46) Wenzler, L.A.; Moyes, G.L.; Raikar, G.N.; Hansen, R.L.; Harris, J.M.; Beebe, T.P., Jr. *Langmuir* **1997**, *13*, 3761–3768.
(47) van der Vegte, E.W.; Hadziioannou, G. *Langmuir* **1997**, *13*, 4357–4368.
(48) Kado, S.; Yamada, K.; Kimura, K. *Langmuir* **2004**, *20*, 3259–3263.
(49) Ito, T.; Citterio, D.; Buhlmann, P.; Umezawa, Y. *Langmuir* **1999**, *15*, 2788–2793.
(50) Vishweshwar, P.; Nangia, A.; Lynch, V.M. *Cryst. Eng. Comm.* **2003**, *5*, 164–168.
(51) Ghosh, K.; Datta, M.; Frohlich, R.; Ganguly, N.C. *J. Mol. Struct.* **2005**, *737*, 201–206.
(52) Auletta, T.; de Jong, M.R.; Mulder, A.; van Veggel, F.C.J.M.; Huskens, J.; Reinhoudt, D.N.; Zou, S.; Zapotoczny, S.; Schonherr, H.; Vansco, G.J.; Kuipers, L. *J. Am. Chem. Soc.* **2004**, *126*, 1577–1584.
(53) Furuta, Ch.; Suzuki, A.K.; Taneda, S.; Kamata, K.; Hayasi, H.; Mori, Y.; Li, Ch.; Watanabe, G.; Taya, K. *Biol. Reprod.* **2004**, *70*, 1527–1533.